[1]Venkata Sai Rahul Trivedi Kothapalli

Navigating the Intersection of AI and Public Health: Challenges and Opportunities

JES Journal of Electrical Systems

Abstract—This paper explores the intricate relationship be- tween artificial intelligence (AI) and public health, highlighting the transformative potential of AI technologies in addressing complex health challenges. This paper discusses various AI ap- plications, including predictive analytics, personalized medicine, and health data management, which enhance disease prevention and patient care. However, the integration of AI in public health also presents significant challenges, such as ethical concerns, data privacy, and the need for interdisciplinary collaboration. The paper aims to provide a comprehensive overview of these dynamics, emphasizing the importance of responsible AI deployment to improve health outcomes while mitigating risks. By examining case studies and current research, the paper offers insights into the future directions of AI in public health, advocating for policies that promote equitable access and effective utilization of AI resources.

Keywords: equitable, improve, concerns, emphasizing

I. INTRODUCTION

Artificial Intelligence (AI) is revolutionizing public health by offering innovative solutions to complex health challenges. From predictive analytics and disease surveillance to personalized medicine and resource optimization, AI enhances the efficiency and effectiveness of public health systems. [1] Its potential to analyze vast datasets in real time enables early detection of outbreaks, risk prediction, and targeted interventions, ultimately improving population health outcomes.

However, the integration of AI into public health is not without challenges. Ethical considerations, data privacy concerns, and the risk of algorithmic bias pose significant barriers to equitable implementation. Additionally, the interdisciplinary nature of public health requires collaboration across diverse sectors to ensure AI technologies are both effective and socially responsible.

This paper explores the duality of opportunities and challenges presented by AI in public health, offering insights into its current applications, limitations, and future potential. [2] By addressing these challenges, this paper aims to advocate for policies and practices that ensure the responsible deployment of AI to promote health equity and improve global health outcomes.

II. PROBLEM DEFINITION

A wealth of scientific evidence underscores the role of human-induced carbon dioxide emissions in accelerating cli- mate change, with potential outcomes that, while uncertain, could be catastrophic. This has intensified societal demand for a faster transition from fossil fuel-based energy systems to those relying on renewable sources. Beyond political and societal drivers, diminishing conventional oil reserves have reduced the effectiveness of oil and gas extraction processes, increased operational costs, and led to the eventual cessation of production and decommissioning of facilities. Consequently, infrastructure such as wells, platforms, processing equipment, and transport pipelines, even if still operational, must be dismantled during abandonment procedures. [3]

Simultaneously, renewable energy capacity is experiencing rapid growth across many regions. For

[1] (Colorado State University), Systems Engineering Department, Fort Collins, CO, USA
Trivedi.Kothapalli@colostate.edu
3waythe@gmail.com

instance, the North Sea region is witnessing the development of numerous wind farms, which are expected to quadruple renewable electricity production. This expanded capacity will exceed Denmark's electricity demand multiple times over. However, the fluctuating and intermittent nature of wind energy prevents it from fully replacing reliable fossil-fuel-based power plants. The transition to a completely renewable energy infrastructure hinges on large-scale energy storage solutions that can act as a buffer, ensuring a stable and continuous power supply to the grid. [4]

This project aims to evaluate the feasibility of repurposing the "to-be-abandoned" North Sea oil and gas fields and their associated infrastructure for large-scale energy storage, addressing the intermittency challenges of wind energy in the region.

The research will address three central questions. Firstly, how much energy storage is required to meet Denmark's needs? Secondly, to what extent can subsurface storage con- tribute to fulfilling this demand? Lastly, which technologies hold the most promise from a technical perspective? This report will provide practical, reproducible methods and quantitative solutions to these questions.

A. Future energy need of Denmark

Currently, Denmark's energy consumption stands at approximately 100 kWh per person per day, distributed across various forms of energy. Eftekhari demonstrated that this energy usage can be divided into three main categories: 30% electricity, 30% heating, and 40% hydrocarbon fuel. Notably, the hydrocarbon consumption allocated for electricity generation is excluded from the 40% hydrocarbon fuel category. Looking ahead, it is reasonable to assume that heating systems and short- distance transportation will transition to electric alternatives. Considering a realistic coefficient of performance for future heating systems, the energy demand can be recalibrated from the current 30-30-40 distribution to approximately 45-40. This corresponds to an estimated demand of 45 kWh/day per person for electricity and 40 kWh/day per person for liquid fuel.

These values will serve as the basis for calculations throughout this report.

Regarding electricity production, Denmark's strategic plan involves a fourfold increase in the electricity generation capacity of offshore wind farms in the North Sea. However, since capacity does not equate to actual electricity output (due to factors like weather variability, curtailment, and technical limitations), this report estimates intermittent wind power generation by scaling Denmark's current electricity production by a factor of four. Data supporting this estimation has been sourced from the Energinet.dk website and is supplemented with electronic attachments, including several MATLAB functions for data analysis and visualization. [5]

Figure 1 illustrates the projected electricity supply and demand for January 2020 (left panel) and January 2050 (right panel). To analyze average supply and demand over different time intervals—ranging from 24 hours to six months—the following equation is applied:

$$E = \frac{1}{t_2 - t_1} \int_{t_1}^{t_2} E(t)\, \mathrm{d}t, \tag{1}$$

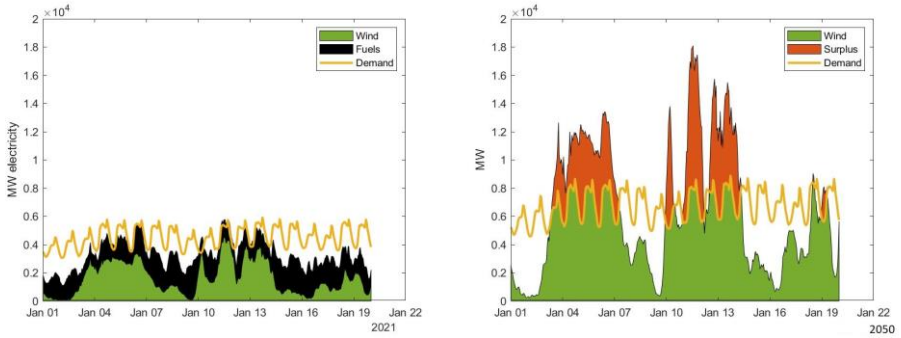

Fig. 1. Comparison of Denmark's electricity supply and demand in January 2020 and projected conditions for January 2050. The left panel illustrates current data, while the right panel depicts future estimates based on wind energy expansion.

where $E(t)$ [MW] represents electricity supply or demand, and t_1 [s] and t_2 [s] define the time interval.

Future energy scenarios are estimated using a scaling factor derived from current data, as expressed in:

$$E_{f\,uure} = \lambda_i E_{current}, \qquad i = s, d \tag{2}$$

where $\lambda_d = 1.5$ reflects a 50% increase in electricity demand, and $\lambda_s = 4.0$ corresponds to a 400% rise in wind farm capacity. This increase is assumed to primarily occur in the offshore sector, although, for simplicity, it is applied to the overall wind energy capacity. Another key assumption in Eq. (2) is that weather patterns in 2050, particularly wind conditions, will be similar to those in 2020.

As shown in Figure 1, there will be periodic mismatches between wind electricity supply and demand, resulting in instances of surplus or shortage. These fluctuations can span durations from several hours to weeks. Figure 2 further visualizes average surpluses and shortages over intervals ranging from 24 hours to eight months, revealing that beyond a six-month period, these values stabilize. This visualization provides three critical insights for 2050: first, the average electricity shortage is projected to be 1.6 GW, representing the power that needs to be stored. On the positive side, the average surplus is estimated at 2.25 GW—620 MW greater than the shortage. These metrics define the requirements for energy storage technology, where the efficiency must exceed:

$$\eta_{storage} > \frac{Average\ shortage}{Average\ surplus} = 0.72,$$

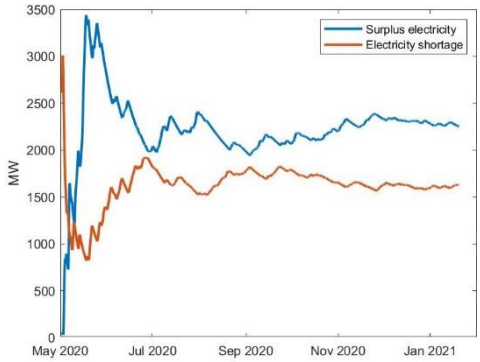

Fig. 2. Visualization of Denmark's average electricity supply and demand between May 2050 and January 2051. Data integration is performed using Eq. (1), showing trends over different time scales.

electricity shortage, which can occasionally exceed the long- term average. These fluctuations are visualized in Fig. 3.

To design an effective storage system, it is essential to accommodate a peak power surplus of 5.0 to 10.0 GW (see the highest points of the left curve in Fig. 3) and retrieve stored energy at a peak rate of 3.0 to 6.0 GW (refer to the right curve in Fig. 3). These peak values are crucial for defining the capacity and specifications of the storage and recovery infrastructure. The subsequent sections will delve into the equipment sizing and process design considerations. [7]

To conclude this section, this paper estimates the subsurface reservoir volume needed to store

sufficient energy to address an eight-month electricity shortfall. Table I summarizes the exergy per mole for various energy storage media analyzed in this study. Exergy, ex_i [kJ/mol], quantifies the usable energy in a system that can be converted into mechanical work, such as electricity or motion. The table also provides the maximum production efficiency, η_i, for each medium.

,For these calculations, the density of stored fluids is indicating that storage systems must achieve an efficiency greater than 72%. [6]

Although the earlier analysis estimates the average storage requirements, the real-time variations in electricity surplus and deficit must also be considered. The actual electricity surplus determined under typical reservoir conditions, T_{res} [K] and p_{res} [bar]. For the chalk reservoirs in the Danish North Sea, conditions of 70^{o}C and 200 bar were assumed. The required reservoir volume is calculated using the following equation:

$$V_{res,i} = \frac{E_{shortage}\, t_{shortage}\, MW_i}{ex_i \rho_i \varphi},$$

that needs storage fluctuates significantly over time, as does the

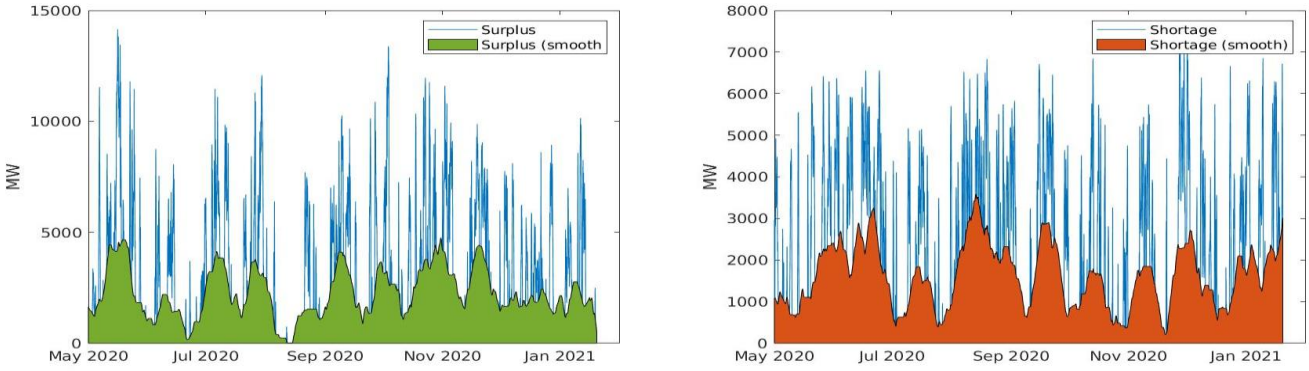

Fig. 3. Projected electricity surplus (left) and deficit (right) for 2050, shown as smoothed curves using an area plot for clarity.

where $\bar{E}_{shortage}$ [kW] represents the average electricity short- fall, $t_{shortage}$ [s] is the duration of the shortage (here assumed as eight months), MW_i [kg/mol] is the molecular weight of the stored fluid, ρ_i [kg/m^3] is the fluid density at reservoir conditions, and φ is the porosity of the reservoir.

Assuming a reservoir thickness of 100 m, the estimated diameter of a chalk reservoir capable of storing energy for an eight-month shortfall in 2050 is shown in Fig. 4. This calculation assumes ideal efficiency (efficiency factor of 1). If efficiency losses are included, the required reservoir volume could be 2 to 3 times larger. Despite these considerations, the necessary reservoir volume is a small fraction of the total available reservoir capacity in the North Sea. A reservoir with a thickness of 100 m and a radius between 100 m and 3000 m (adjusted for efficiency factors) would suffice to store enough energy to mitigate Denmark's electricity shortfall in 2050 for eight months.

TABLE I Exergy values, production efficiencies, and thermodynamic properties of various energy storage media at reservoir conditions (70o C, 200 bar). Efficiency factors are considered FOR ELECTRICITY-TO-FUEL CONVERSION ONLY.

Component	ρ [kg/m^3]	ex [kJ/mol]	$Vres$ [10^6 m^3]	η [-]
H_2O_2	1,090.0	450	2.30	0.50
C_2H_6	544.0	750	1.80	0.42
O_2	88.8	210	5.00	0.65
C_3H_8	492.0	820	1.75	0.38

N_2	806.0	20.5	60.50	1.0

III. CHEMICAL AND PHYSICAL ENERGY STORAGE

The extraction of oil and gas from the Danish sector of the North Sea has been steadily declining, leading to the eventual shutdown of production and decommissioning of infrastructure, including well closures and facility removals. Concurrently, the operational and planned offshore wind farms in the North Sea are poised to provide a significant supply of low-cost electricity. However, the intermittent nature of wind energy remains a critical challenge.

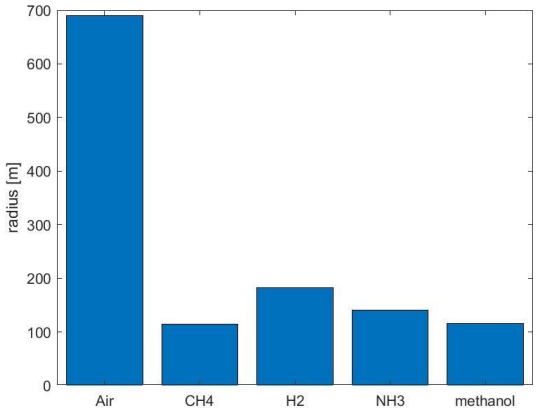

Fig. 4. Estimated diameter of a 100 m thick chalk reservoir required to store fuel equivalent to an eight-month electricity shortfall in 2050, assuming ideal efficiency for all conversion processes.

This chapter proposes that surplus electricity generated during high wind conditions and periods of low demand could be transformed into chemical energy (e.g., hydrogen, ammonia, methanol, or methane) and stored within the extensive depleted oil and gas reservoirs beneath the North Sea. These reserves could then serve as carbon-neutral energy sources, either for use in transportation or for reconversion to electricity during periods of low wind availability.

The chapter evaluates the technical and thermodynamic vi- ability of using offshore facilities to convert excess electricity into storable chemical fuels. The technical assessment examines whether the existing infrastructure, including platforms, pipelines, and surface facilities, can support the necessary equipment for these conversions. [8]

Key processes such as the separation of nitrogen and carbon dioxide from the atmosphere, seawater electrolysis, and the re- duction of CO_2 and N_2 to produce synthetic fuels are modeled using the Aspen Plus process simulator. These simulations are employed to determine equipment sizes and estimate the space requirements for the platforms.

From a thermodynamic perspective, the study measures the exergy losses that occur during the conversion of electricity to chemical fuels and back. It also assesses the storage and retrieval of chemical energy within subsurface reservoirs. This analysis relies on an internally developed open-source dynamic model, which simulates the complex, multi-component, and*2) Carbon Dioxide:* Carbon dioxide, present in the atmosphere at a concentration of approximately 40 ppm, can theoretically be separated using energy equivalent to its chemical exergy:

$$ex_{CO_2} = -RT_{00} \ln x_{CO_2},$$

where R is the universal gas constant (8.314 J/(mol·K)), T non-isothermal fluid flow behavior within the subsurface.$_{\circ}^{00}$

A. *Storage of Synthetic Fuels*

The process of converting electricity into carbon-neutral fuels, often referred to as power-to-X

(P2X), e-refinery, or similar terms, has been a topic of significant research interest. For synthetic fuels to be carbon-neutral, the raw materials must be derived directly from natural sources, such as the atmosphere and seawater. These sources are described as being in the "dead state" in thermodynamics, representing a baseline composition of Earth's atmosphere, crust, and oceans with no inherent capacity to perform work.

This subsection explores the production of key synthetic fuels, including hydrogen, ammonia, methane, and methanol. The raw materials required for these fuels—air and seawater—are processed using surplus electricity generated by wind farms. The production involves separating nitrogen and carbon dioxide from the atmosphere and extracting hydrogen through the electrolysis of seawater. These processes are described in greater detail in the subsequent sections. [9], [10]

B. Nitrogen and Carbon Dioxide from the Atmosphere

1) Nitrogen: Nitrogen can be obtained from air through cryogenic distillation. In this process, shown in Fig. 5, air is first filtered, compressed, and cooled to a liquid state using heat exchangers. The liquid air is then fed into high- pressure and low-pressure distillation columns to separate nitrogen based on differences in boiling points. The nitrogen is collected from the top of the low-pressure column.

This process is highly energy-intensive, requiring a utility stream at approximately -200°C, which is typically provided by the rapid expansion of a compressed refrigerant. The energy consumption for separating nitrogen is reported to vary based on heat integration efficiency, with values ranging from 15 kJ/mol to 32 kJ/mol. The simulation estimates a requirement of 32 kJ/mol, likely reflecting the simplified heat integration in the model. [11]

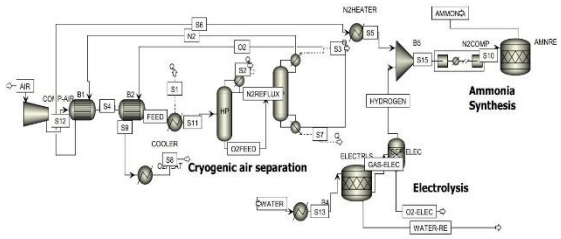

Fig. 5. Schematic of ammonia production using electrolysis and cryogenic air separation.

is the dead state temperature (288.15 K or 15 C for the North Sea), and x_{CO2} is the atmospheric CO_2 mole fraction. This equates to approximately 20 kJ/mol.

In practice, the process efficiency is low, with typical energy requirements of 400 kJ/mol or around 10 MJ/kg CO_2 when considering industrial-scale separation. Additionally, the footprint for direct air capture (DAC) equipment is substantial, ranging from 0.5 to 2 km^2 per million tons of CO_2 captured annually, making offshore deployment impractical.

Alternative sources for CO_2 include biomass or industrial emissions from sectors such as steel, cement, or fossil fuel plants, which are often more accessible onshore. These approaches can be considered carbon-neutral if implemented within a closed cycle. However, these onshore sources are beyond the scope of offshore applications.

C. Production and Storage of Hydrogen

Advances in electrolysis technology have significantly im- proved the efficiency of hydrogen production from water. When powered by wind-generated electricity, the hydrogen produced is a zero-emission fuel. Hydrogen features prominently in energy transition plans for the North Sea region.

Key challenges for offshore hydrogen production and storage include:

- Integration of water treatment, electrolysis, and compression systems on offshore platforms.
- Ensuring the integrity of pipelines for storage and transport.
- Addressing interactions between hydrogen, formation fluids, and chalk reservoirs.
- Assessing the capacity of reservoirs for hydrogen storage and its flow dynamics.
- Evaluating the overall energy efficiency and economic feasibility of the process.

This study specifically addresses energy requirements, equipment sizing, and the behavior of hydrogen flow within chalk reservoirs.

1) Production of Green Hydrogen: Hydrogen can be generated through water electrolysis using the following reaction:

$$2H_2O \rightarrow 2H_2 + O_2$$

The minimum energy required for this process corresponds to the Gibbs free energy change, with approximately 39 kWh of electricity needed per kilogram of hydrogen. However, modern technology typically requires closer to 48 kWh per kilogram of hydrogen.

The hydrogen stream is purified by cooling to 308 K using cooling water, which removes moisture from the hydrogen. Condensed water is recycled back into the process. Residual

moisture in the hydrogen is removed in intercoolers during compression stages. The process requires direct current (DC) electricity, resulting in an approximate 2.5% loss during AC- to-DC conversion. According to Rosen, the exergy efficiency of water electrolysis for mature technologies can reach around 70%, excluding other losses. Details on water treatment and purification were not addressed in this earlier analysis.

Two mature commercial technologies for hydrogen pro- duction include alkaline electrolysis and polymer electrolyte membrane (PEM) cells. When powered by renewable electricity sources, the resulting hydrogen is referred to as “green hydrogen.” These processes achieve efficiencies of about 60% to 70

The concept of storing hydrogen in subsurface reservoirs is not new. Petrochemical plants have historically utilized salt caverns to store large hydrogen volumes. Current research is expanding into subsurface storage options for green hydrogen across various continents.

Recently, several green hydrogen projects have been announced. For example, Ørsted’s H2RES initiative, supported by the Danish Energy Agency’s EUDP program, involves building a 2 MW hydrogen production unit by the end of 2021. This system is expected to produce up to 1,000 kilograms of green hydrogen daily. While this is a step forward, it falls short of addressing the gigawatt-scale energy shortfalls anticipated due to renewable energy intermittency, as highlighted in Chapter II.

Another significant challenge is the spatial footprint of electrolysis equipment. As discussed in Chapter II, synthetic fuel production facilities require gigawatts of surplus electricity. Current electrolysis units are typically designed for megawatt- scale production. For instance, NEL Hydrogen offers commercial PEM electrolyzes with a 25 MW capacity requiring

an area of 3×12 m^2. A 500 MW plant composed of 20 such units would be challenging, albeit not impossible, to fit

on an offshore platform alongside other equipment. A more practical solution could involve using specialized ships to house electrolysis units, or alternatively, conducting hydrogen production onshore.

Finally, converting stored hydrogen back into electricity presents challenges. Pure hydrogen cannot

currently be used as fuel in existing gas turbines, requiring blending with hydro- carbons like methane. This blending introduces carbon dioxide emissions unless carbon capture systems are employed, which reduce overall efficiency. While platforms can accommodate gas turbines up to hundreds of megawatts, gigawatt-scale turbines remain impractical due to space and weight constraints. For instance, a 25 MW offshore turbine capable of burning hydrogen-methane mixtures weighs approximately

250 tones. Platforms can host several such turbines, but achieving gigawatt capacities is a significant hurdle.

D. Methane Production

Methane production involves the catalytic conversion of carbon dioxide (CO_2) and carbon monoxide (CO) using the methanation process, first proposed by Sabatier and Sanderson.

The process begins by capturing CO_2 from natural or industrial sources or by generating a mixture of CO_2 and CO through combustion of hydrocarbons (e.g., fossil fuels) or carbohydrates (e.g., biomass).

At elevated temperatures and in the presence of water vapor, a combination of CO and hydrogen (H_2) is produced. Hydrogen then reacts with CO_2 and CO to form methane in what is known as the Sabatier reaction:

$$CO_2 + 4H_2 \rightarrow CH_4 + 2H_2O$$

This reaction holds promise for converting captured carbon into a storable, energy-dense fuel. Methane's potential applications, along with its production process, are explored further in this study.

$$CO_2 + 4H_2 \leftrightharpoons CH_4 + 2H_2O \qquad \Delta H_0 = -165\ kJ/mol. \quad (3)$$

When the reactants—hydrogen and carbon dioxide—are derived from natural resources like seawater and air using renewable energy, the resulting methane is sustainable and carbon-neutral. The reaction is typically catalyzed using nickel or ruthenium in a packed bed reactor. Various studies report the reaction rates under different pressures and temperatures. While side reactions may occur under the elevated conditions of methanation reactors, methane formation is highly selective.

Nearly complete methane selectivity, approaching 100

A conceptual diagram of green methane production is shown in Fig. X. In this setup, hydrogen is obtained via water electrolysis, and carbon dioxide is captured from the air. Alternative carbon sources, such as biomass or CO_2 emissions from industrial activities (e.g., steel or cement production), can also be used. However, atmospheric CO_2 capture ensures the resulting methane is carbon-neutral, making it "green." The reactor operates at pressures between 20 and 70 bar and temperatures ranging from 473 to 673 K.

The efficiency of the overall methane production process can be determined by the following formula:

$$\eta_{methane} = \frac{ex^{ch}_{CH_4}}{4\frac{ex^{ch}_{H_2}}{\eta_{electrolysis}} + \frac{ex^{ch}_{CO_2}}{\eta_{capture}} + \frac{ex_{compression}}{\eta_{comp}\,\eta_{driver}\,\eta_{transmission}}}, \quad (4)$$

where ex^{ch}_i (kJ/mol) represents the chemical exergy of com- ponent i, and η_j denotes the efficiency of process j. The term $ex_{\text{compression}}$ (kJ/mol methane) accounts for the exergy required to compress hydrogen and CO_2 to the reactor pressure in a multi-stage compressor.

As the reaction is exothermic, the heat released is assumed to sustain the reactor's temperature at 673

K. Using the energy calculations for compression outlined in Section **??** and ap- plying the efficiencies defined in earlier sections, the methane production efficiency is calculated to be $\eta_{\text{methane}} = 36\%$. This is significantly lower than the anticipated value of 72

Additionally, this process requires a substantial physical footprint to facilitate atmospheric CO_2 capture and water electrolysis. Therefore, it may not be a viable solution for addressing wind energy intermittency in Denmark. However, the process can be adapted for offshore platforms if hydrogen and CO_2 are supplied via pipelines. Under these conditions, platform-based operation is feasible.

E. Ammonia

Ammonia synthesis involves a catalytic exothermic reaction between nitrogen and hydrogen, as represented by the following equation:

$$N_2 + 3H_2 \rightarrow 2NH_3.$$

This process is typically conducted in a reactor operating at pressures of approximately 200 bar and temperatures ranging from 300°C to 500°C. Nitrogen and hydrogen, the primary feedstocks for ammonia production, are derived from air and seawater, respectively. Nitrogen is separated via cryogenic air separation, while hydrogen is produced through water electrolysis. Both gases are compressed to pressures between 150 and 250 bar and fed into a packed bed reactor operating between 673 K and 773 K.

The reaction releases heat, eliminating the need for external heating. This high-temperature heat can be harnessed for other stages of the process. While the ammonia production unit can be accommodated on an offshore platform, the hydrogen electrolysis units required for GW-scale hydrogen production are too large to fit. Similarly, the cryogenic air separation unit for nitrogen, although feasible, poses challenges due to the need for long and heavy distillation columns (e.g., 60 theoretical trays) operating at extremely low temperatures. to consume extra hydrogen molecules to eliminate oxygen atoms, as is required when carbon dioxide serves as a reactant.

F. Methanol

Methanol is produced through a catalytic process involving hydrogen and carbon dioxide, following the reaction:

$$CO_2 + 3H_2 \rightarrow CH_3OH + H_2O \quad (6)$$

The reactor operates at a pressure of 100 bar and a temperature of 264°C. Since the reaction is exothermic, cooling is required to maintain optimal operating conditions. This is typically achieved by circulating water, which absorbs the heat and generates steam. To facilitate the reaction, the material streams entering the reactor are compressed to pressures between 50 and 100 bar. These columns affect platform stability and require significant space for utilities.

While the chemical exergy of methanol is lower than that of methane, the synthesis of methanol proves to be slightly more energy-efficient. This is primarily because the reduction of CO_2 to methanol produces only one molecule of water per molecule of methanol, compared to methane production, where two molecules of water are generated per methane molecule. As a result, methanol production is more efficient in terms of exergy recovery.

Similar to the production of methane and ammonia, the efficiency of methanol synthesis can be evaluated by the following equation:

$$\eta_{\text{methanol}} = ex^{\text{ch}}_{\text{CH}_3\text{OH}} \left(\frac{3\text{ex}^{\text{ch}}_{\text{H}_2}}{\eta_{\text{electrolysis}}} + \frac{\text{ex}^{\text{ch}}_{\text{CO}_2}}{\eta_{\text{capture}}} + \frac{\text{ex}_{\text{compression}}}{\eta_{\text{comp}}\,\eta_{\text{driver}}\,\eta_{\text{transmission}}} \right)^{-1}, \quad (7)$$

To address these limitations, an alternative design is pro- posed. Instead of cryogenic separation,

nitrogen is generated by burning hydrogen with air in a gas turbine. The resulting mixture of nitrogen and steam is then separated in a two-phase separator, where steam condenses. The separated nitrogen can either be used in a secondary Rankine cycle to generate additional work or compressed in a multistage compressor and directed to the ammonia reactor. In the reactor, compressed nitrogen reacts with hydrogen to produce ammonia.

The efficiency of this alternative process is calculated as:

$$\eta_{\text{ammonia}} = \frac{\text{ex}^{\text{ch}}_{\text{NH}_3}}{\left(1.5 + \frac{0.21}{0.79}\right)\frac{\text{ex}^{\text{ch}}_{\text{H}_2}}{\eta_{\text{electrolysis}}} + \frac{\text{ex}_{\text{compression}}}{\eta_{\text{comp}}\,\eta_{\text{driver}}\,\eta_{\text{transmission}}} - \text{ex}_{\text{turbine}}},$$

The estimated efficiency for methanol production is around 40%, reflecting the combined losses in the electrolysis, CO_2 capture, and compression stages.

However, storing methanol in the subsurface is not recommended. This is due to the fact that methanol can be broken down by subsurface microorganisms, potentially leading to losses. Consequently, methanol is excluded from the subsurface storage model. If desired, modifications to the MATLAB script can be made to include methanol, but microbial degradation would need to be excluded from the energy efficiency calculations.

(5) where the factor 0.21/0.79 accounts for the proportion of hydrogen consumed during combustion to separate oxygen from nitrogen in the air.

This redesigned process achieves an efficiency of 43

It is important to note that current gas turbines cannot operate on pure hydrogen, so this process relies on advancements in turbine technology.

Among all considered fuels, ammonia boasts the highest synthesis efficiency due to the relatively low energy required for nitrogen separation. Additionally, ammonia formation directly combines hydrogen and nitrogen without the need Compressed Air Storage

Compressed air energy storage (CAES) is an established and effective technology for storing electricity during periods of low demand. In the United States, large storage tanks are used to compress air when electricity is inexpensive and then release it to generate power during peak periods. Although the efficiency of CAES is not particularly high, its economic feasibility is supported by electricity pricing schemes that incentivize consumers to shift their usage to off-peak times.

The idea of large-scale electricity storage in the subsurface emerged as a way to reduce wasted energy from fossil fuel power plants. These plants, designed for continuous operation, often suffer efficiency losses when forced to operate below their optimal capacity. Shutting down these plants is costly and inefficient due to the long and expensive startup times. Therefore, compressed air storage offers a solution by storing surplus energy when demand is low and releasing it during peak demand, helping to balance electricity supply and de- only one water molecule per methanol molecule, in contrast to methane synthesis, which yields two water molecules per methane. Consequently, methanol production offers slightly higher efficiency in exergy utilization.

The energy efficiency of methanol production can be deter- mined using the following expression:

$$\eta_{\text{methanol}} = ex^{\text{ch}}_{\text{CH}_3\text{OH}}\left(\frac{3\text{ex}^{\text{ch}}_{\text{H}_2}}{\eta_{\text{electrolysis}}} + \frac{\text{ex}^{\text{ch}}_{\text{CO}_2}}{\eta_{\text{capture}}} + \frac{\text{ex}_{\text{compression}}}{\eta_{\text{comp}}\,\eta_{\text{driver}}\,\eta_{\text{transmission}}}\right)^{-1}, \quad (9)$$

mand. This concept can also be applied to offshore wind farms,
using decommissioned gas fields as storage reservoirs.

A schematic diagram of compressed air energy storage is provided in Fig. 7, which is similar to other gas storage processes. In CAES, air is injected into underground reservoirs via compressors. As the input power fluctuates, the efficiency of the compression process varies because compressors do not always operate under optimal conditions. During times of electricity deficit, the compressed air (or other gases such as hydrogen or methane) is released and passed through a gas turbine, which powers a generator to produce electricity.

When assuming negligible losses due to friction and heat in the reservoirs and wells, the theoretical efficiency of this process can reach up to 50%. This is simply the product of the efficiencies of the compressor and gas turbine. However, during dynamic operation, factors such as variable power input, friction, and heat losses reduce the overall efficiency, which will be explored further in the next chapter.

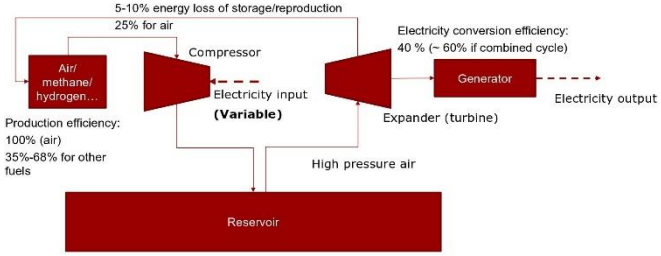

Fig. 6. A block flow diagram depicting the subsurface gas storage process, highlighting key efficiency factors.

G. Methanol

Methanol is synthesized through a catalytic reaction be- tween hydrogen and carbon dioxide, represented by the equation:

$$CO_2 + 3H_3 \rightarrow CH_3OH + H_2O \quad (8)$$

The reactor operates under conditions of 100 bar pressure and a temperature of 264°C. As the process is exothermic, cooling measures are essential to maintain the reactor's temperature within safe limits. This is typically achieved by circulating water, which absorbs excess heat and converts it into steam. The reactant streams entering the reactor are compressed to pressures ranging from 50 to 100 bar to facilitate the reaction.

Although the chemical exergy of methanol is lower than methane's, methanol production tends to be more efficient in terms of energy recovery. This is due to the fact that the CO_2 reduction to methanol results in the production of the estimated efficiency of methanol production is approximately 40%, which accounts for the combined losses in the electrolysis, CO_2 capture, and compression processes.

Storing methanol in subsurface reservoirs is not advisable, as methanol can be degraded by microorganisms found underground, leading to potential energy losses. As a result, methanol is excluded from the subsurface storage model. However, if necessary, modifications to the MATLAB script could be made to include methanol, though microbial degradation must be excluded from the energy efficiency calculations.

H. Compressed Air Storage

Compressed air energy storage (CAES) is a proven technology for storing surplus electricity during times of low demand. In the United States, large tanks are used to compress air when electricity is less expensive, and the stored air is then released to generate power during periods of high demand. While CAES is not highly efficient, its economic viability is supported by electricity pricing

schemes that encourage consumers to shift their usage to off-peak periods.

The concept of subsurface energy storage emerged to ad- dress the inefficiencies of fossil fuel power plants that are designed for continuous operation. These plants often experience efficiency losses when operating below their optimal capacity. Shutting down such plants is not practical due to the high cost and time required to restart them. Compressed air storage helps mitigate this issue by storing excess energy when demand is low and discharging it during peak demand to balance the electricity grid. This concept can also be applied to offshore wind farms, where decommissioned gas fields serve as storage reservoirs.

A schematic of compressed air energy storage is shown in Fig. 7, which is similar to other gas storage processes. In CAES, air is compressed and injected into underground reservoirs. As the input power fluctuates, the efficiency of the compression process also varies, since compressors do not always operate under optimal conditions. When electricity demand exceeds supply, the compressed air (or other gases like hydrogen or methane) is released and passed through a gas turbine, which powers a generator to produce electricity. In an idealized scenario where friction and heat losses in the reservoirs and wells are neglected, the theoretical efficiency of this process can reach up to 50%. This is the result of multiplying the efficiencies of the compressor and the gas turbine. However, in practice, the efficiency decreases due to dynamic operational conditions such as variable power input, frictional losses, and heat dissipation, which will be discussed in further detail in the next chapter.

[m] and R_{zone} [m], respectively. The fluid injection rate is determined by the surplus electricity available and the conversion efficiency of the synthetic fuel (or compressed air) generation process. The total injection rate is given by:

$$qin = \frac{E_{excess}\,\eta_m\,MW_m}{\pi D_{wellbore}\,H_{strat}\,ex_m^{phys}\,\rho_m}$$

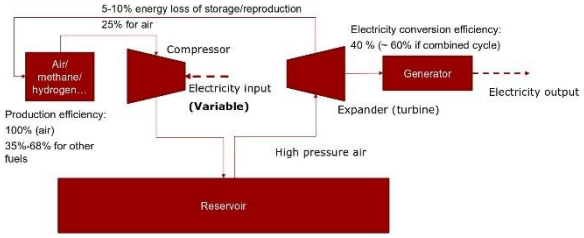

Fig. 7. A block flow diagram illustrating the subsurface gas storage process and the key efficiency factors.

where ρ_m [kg/m^3] is the density of the synthetic fuel m, calculated at the bottom hole pressure and the injection temperature, which is assumed to be nearly equal to the reservoir's temperature. The bottom hole pressure is deter- mined iteratively through a trial-and-error process, matching the reservoir model with the injection boundary condition derived from the above equation.

For compressed air, the chemical exergy ex^{phys} [kJ/mol] $_m$

TABLE II Representative efficiency values for different energy system components

Device	Compressor	Electrical Driver	Electricity Trans- mission
Efficiency Factor (%)	75	85	98

IV. SUBSURFACE ENERGY STORAGE SOLUTIONS

Energy can be stored in a variety of underground geological formations, typically classified into two broad types: sandstone formations (e.g., Redwood Field) and limestone formations (e.g., Silverstone). The Redwood Field is a sandstone gas reservoir located at a depth of roughly 3200 meters, with an operating temperature of around 125°C. It has a porosity of 0.19, with permeability values ranging from 3 to 45 mD across its layers. The two most conductive layers, with permeabilities of 12 and 48 mD, have an estimated combined thickness of about 105 meters. On the other hand, the Silverstone limestone reservoir is situated 1900 meters below the surface, with an average porosity of 0.30 and permeability of 2.8 mD. Vertical wells are typically drilled in sandstone reservoirs like Redwood Field, while horizontal wells are more commonly employed in limestone deposits such as Silverstone.

For vertical wells, this paper assumes the reservoir thickness is approximately 110 meters, which results in a storage zone radius ranging from 120 to 950 meters around the well. For horizontal wells, the energy storage area is generally smaller. It is assumed that all wells, whether for storage or extraction, have a diameter of 5 inches. The layout of the reservoir system is illustrated in Fig. [Insert figure reference].

A. *Development of the Storage Model*

The reservoir is represented as a cylindrical system, with the upper and lower boundaries sealed to prevent any fluid flow through them. The outer boundary of the reservoir can either be sealed or maintained at hydrostatic pressure. The top surface of the reservoir is located at a depth of D [m], with the thickness of the reservoir represented by H_{strat} [m], while the well and reservoir radii are denoted by $0.5D_{wellbore}$ is substituted with the physical exergy of the compressed air, which is calculated based on the bottom hole pressure using a similar trial-and-error method. The energy required for gas compression during injection is based on an injection pressure defined as $p_{comp} = p_{bh} + \Delta p_{line}$, where p_{bh} [Pa] represents the bottom hole pressure, and Δp_{line} [Pa] is the pressure drop within the pipeline, which is calculated using the Aspen Plus "pipe" unit.

For the period between October 1st and December 1st, it is assumed that the fluids are simply stored in the subsurface while surplus electricity is available. After this storage phase, depending on the electricity supply-demand balance, the system may shift to storage or production phases. The extracted fluid is used to meet electricity shortages. Therefore, the withdrawal rate is directly governed by the demand for electricity. If the withdrawal rate surpasses the reservoir's capacity to supply, the bottom hole pressure may fall below zero, causing a system failure. To avoid such issues, it would be useful to estimate the reservoir's maximum production capacity using an analytical model, though this approach has not been incorporated into the current version of the model.

B. *Modeling Subsurface Energy Storage*

In the context of storing synthetic fuels and compressed air within subterranean gas reservoirs, I utilize a model that simulates multi-component, single-phase flow. Gas storage in water-flooded reservoirs is less efficient due to the trapping of gas by capillary forces, which causes a permanent storage of much of the gas. Although techniques like superheated steam or hot gas injection can be applied to dry out the reservoir and prepare it for gas injection, these methods are highly energy-demanding and may result in thermally-induced fractures. Hence, the paper focus is on using gas reservoirs for storing energy carriers in their gaseous state. For storing liquid-phase energy carriers, I consider both gas and oil reservoirs. In both cases, the paper model incorporates the compressibility of fluids, which is a key factor influencing the extraction process.

The primary equation that governs the flow of compressible fluids in a single-phase system within

porous media is:

$$\frac{\partial}{\partial t}(\phi\rho) + \nabla .(\rho v) = 0, \tag{10}$$

where Darcy's velocity for single-phase flow, assuming negligible gravitational effects, is given by:

$$v = -\frac{k_s}{\mu_f}\nabla\rho, \tag{11}$$

The equation governing advection-diffusion, which models the flow of synthetic fuel through the subsurface, is:

$$\frac{\partial}{\partial t}(\phi c_f) + \nabla \cdot (v c_f - \phi D_f \nabla c_f) = 0. \tag{12}$$

the bottom-hole pressure remains above a specified threshold. This guarantees efficient turbine operation. It is assumed that the gas turbine maintains a steady efficiency of 90%, mirroring that of the injection compressor, with the performance of both systems unaffected by fluctuating operational conditions or external variables.

For the simulation, I assume a total of 25 MW of surplus electricity is directed toward the compressed air storage system located in the Harald West field. During the storage phase, the injected air is stored at a pressure of 200 bar, which in these equations, ϕ [-] denotes porosity, k_s [m^2] is the permeability, ρ [kg/m^3] represents the fluid density, p [Pa] is the reservoir pressure, μ_f [Pa.s] is the fluid viscosity, D_f [m^2/s] is the diffusivity of synthetic fuel, and c_f [mol/m^3] is the concentration of the synthetic fuel. The viscosity and density are both functions of the fuel concentration. As previously mentioned, the rate of fluid injection at the well is determined by the available electricity, based on surplus electricity data from the year 2020, with projections for 2050. These equations are solved numerically using the finite volume method, with spatial discretization handled by FV Tool, a MATLAB-based tool, in a two-dimensional, axisymmetric (cylindrical) coordinate system. Different permeability fields are modeled, including high-permeability zones near the well. A modified version of the model, which includes fractures, has also been implemented. A permeability field corresponding to the Harald West field, including a stimulated zone near the well, is depicted in Fig. 9.

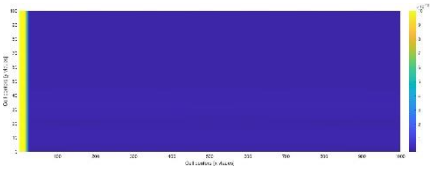

Fig. 8. Permeability field utilized in simulating compressed air and ammonia injection in the Harald West reservoir, where the permeability near the well is 100 times higher than the average permeability of the reservoir.

C. Results and Evaluation

This section presents the results derived from the simulations of compressed air and ammonia-based energy storage systems within the Harald West gas reservoir. The permeability distribution within the reservoir is illustrated in Fig. 9, where an enhanced stimulation treatment has been applied around the wellbore, creating a high-permeability zone with a radius of 25 meters. The permeability in this

region is 150 times greater than the average value found in the unaltered reservoir. This stimulation is critical for managing the large fluid flow rates needed for energy storage operations on the scale of tens of megawatts to gigawatts.

The energy withdrawal phase commences on January 1st, 2051, in response to an electricity deficit. To ensure the gas turbine installed on the platform can compensate for pressure losses within the well, the withdrawal rate is adjusted so that is necessary for effective energy storage. The injection rate is managed according to the reservoir's capacity to maintain pressure while balancing the available electricity. The model also considers the potential impact of reservoir heterogeneity, including the presence of lower-permeability layers that can limit fluid flow and require optimized well placement.

In addition to the performance of the storage system, I evaluate the economic implications of the system's scale. Based on current energy prices and technological assumptions for 2050, the cost of compressing and storing 1 MWh of electricity in the form of compressed air is estimated at $50. This cost includes energy losses due to compression and friction in the injection wells, as well as the cost of maintenance for the underground storage facilities. This cost is expected to decrease by up to 30% with advances in compressor technology and pipeline efficiency over the next two decades.

The simulations indicate that ammonia storage systems offer potential advantages over compressed air in terms of energy density and long-term storage stability. The ammonia-based systems, when scaled appropriately, can offer higher efficiency in terms of energy recovery during the withdrawal phase, making them a promising alternative for regions with extensive storage requirements like the North Sea.

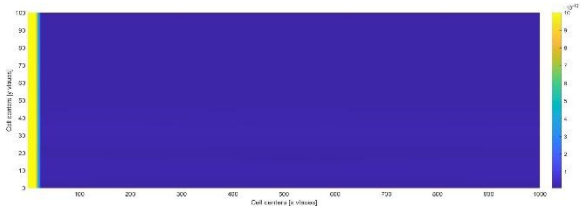

Fig. 9. Permeability distribution used for modeling compressed air and ammonia injection within the Harald West reservoir. The high-permeability zone, induced by wellbore stimulation, extends for 25 meters with a permeability 150 times that of the surrounding reservoir material.

D. Compressed Air Energy Storage

Figure 10 illustrates the pressure history at the bottom of the well. This pressure profile is essential for evaluating the overall efficiency of the energy recovery process, comparing the electricity produced with the amount of surplus power used for injecting compressed air from October to January 2050. The findings reveal that only a mere 1.6% of the 20 MW of electricity consumed during the injection phase is recovered through the compressed air storage system, indicating a very low recovery efficiency. Additionally, the pressure within the reservoir rises significantly, surpassing the hydrostatic pressure

multiple times, though this increase is confined to a small region around the injection well. This sharp rise in pressure, along with rapid fluctuations (as much as 1000 bar within a few hours or days due to variability in wind power generation), poses a risk of geomechanically instability within the reservoir. Consequently, it is advisable to limit the surplus electricity storage to smaller quantities using a single vertical well. The tracer distribution, as shown in Fig. 11, reveals that after four months of operation, the tracer has only diffused to a distance of 700 meters from the well. This suggests that an alternative, more controlled storage option, such as a salt cavern, could be more effective. Salt caverns would offer similar storage capacity without the complexities associated with

fluid flow through porous media, particularly at pressures exceeding several hundred bars.

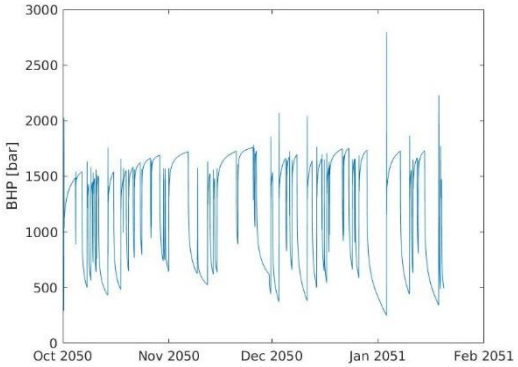

Fig. 10. Pressure changes at the wellbore following the injection of com- pressed air from October to December 1st, 2050, before storage and extraction.

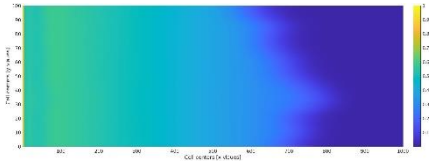

Fig. 11. Tracer dispersion after four months of compressed air injection and extraction in the Harald West reservoir.

The low efficiency in energy recovery can be better under- stood by analyzing the pressure data shown in Fig. 12. In the region near the well, pressure drops quickly due to a high extraction rate. However, the flow from the first 100 meters of the reservoir to the enhanced zone is hindered by the low permeability of the surrounding rock, despite the overall pressure remaining high (above 600 bar). To better understand the limitations and optimize the process, a more comprehensive analysis using an analytical model could be useful. This model would help determine the maximum practical injection and extraction rates for compressed air storage systems. A script for calculating pseudo-pressure, available in the supplementary MATLAB files, has been developed to assess the potential of gas fields for use in compressed air energy storage systems.

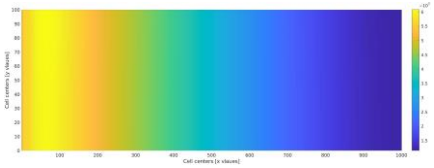

Fig. 12. Pressure distribution following the injection and production of compressed air in the Harald West field.

E. Ammonia Storage

In the previous discussion, I saw that compressed air storage, due to its lower exergy value (energy available for work), demands significantly larger volumes and extremely high injection/extraction rates, leading to unmanageably large pressure differentials in the reservoir. [12] To address these challenges, a more energy-dense medium, such as ammonia, can be used for storage. For the purpose of this analysis, I allocate 100 MW of surplus electricity to the production and storage of ammonia at the Harald West facility, which is five times the power requirement of the compressed air storage system. As depicted in Fig. 13, [13] the pressure during ammonia injection only rises 150 bar above the hydrostatic baseline, staying within acceptable limits. However, the pressure does fluctuate between 200 and 350 bar, which could potentially risk geomechanically failure in the reservoir, warranting further investigation.

Similar to compressed air storage, the production rate during ammonia extraction is limited by the reservoir's low permeability, as shown in Fig. 14. To prevent negative pressures in the wellbore during withdrawal, a limit is imposed on the extraction rate—capped at 20% of the maximum injection rate. With this restriction in place, the efficiency of converting stored ammonia back into electricity (assumed to be 60% efficient) is only 2.3%. Though this marks an improvement compared to compressed air storage, it still fails to meet the 72% efficiency benchmark, which is required for an effective solution to address the intermittency of energy from North Sea wind farms.

Figure 15 illustrates the normalized ammonia concentration in the reservoir after four months of storage and withdrawal. After this period, the ammonia has spread to a radius of 300 meters from the injection well. In regions of lower pressure, where recovery is not feasible, the concentration shows a loss of approximately 30% of the injected ammonia. This indicates that the majority of the ammonia remains in the reservoir, and I anticipate that losses will primarily occur during the early stages of storage as the reservoir is pressurized in preparation for later extraction.

Additionally, I ran simulations for injecting both com- pressed air and synthetic fuels into a horizontally oriented well. Although the pressure profile for these simulations is somewhat different—showing much less fluctuation, particularly for the enhanced wells—the overall energy efficiency remains consistent. This finding suggests that for optimal subsurface energy storage, whether for physical or chemical

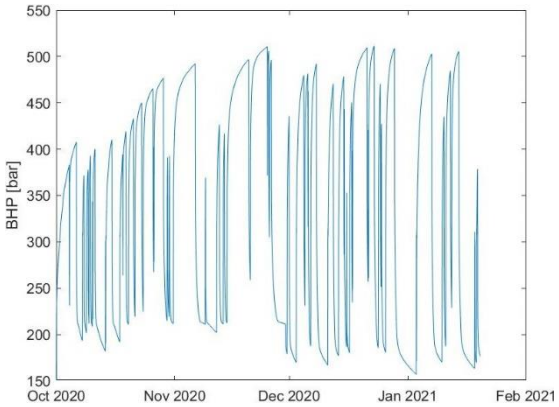

Fig. 13. Pressure history at the bottom of the ammonia storage well at the Harald West site.

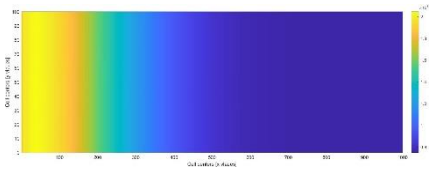

Fig. 14. Pressure distribution within the reservoir at the conclusion of four months of ammonia injection and extraction.

energy, confined storage spaces like salt caverns are likely more effective than large, diffusive reservoirs, where fluid dispersion can reduce the efficiency of the energy storage process.

V. CONCLUSIONS AND RECOMMENDATIONS

This research investigates the feasibility of utilizing sub- surface storage for surplus electricity generated by North Sea wind farms, focusing on both physical energy (compressed air) and chemical energy (synthetic fuels). These energy storage systems are critical to addressing the intermittency of renew- able wind power. Based on the results of this study, several key findings and

recommendations have emerged:

1) A successful energy storage system must limit energy losses to below 30%. Currently, hydropower and battery storage technologies are the most efficient, though hydropower's reliance on specific geographic locations and batteries' scalability limitations restrict their applicability. Among synthetic fuels, green hydrogen, under optimal conditions, holds promise for meeting this efficiency threshold.

2) By 2050, the electricity storage demand is projected to exceed 1000 MW. While hydrogen electrolysis systems are advancing, current commercial systems are limited to 20 MW, making them unsuitable for large-scale offshore applications. Additionally, the lack of dedicated hydrogen turbines and the need to blend hydrogen with hydrocarbons for combustion further complicates its use.

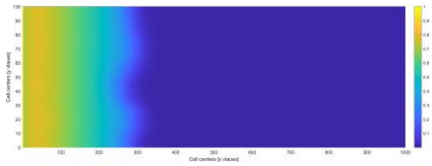

Fig. 15. Ammonia concentration distribution after four months of ammonia storage and extraction at the Harald West facility.

3) Both methane and methanol require substantial carbon sources for their production, such as CO_2. Capturing CO_2 directly from the atmosphere is highly energy- intensive, undermining the overall efficiency of these fuels. Furthermore, their large physical footprint poses challenges for offshore integration. However, capturing CO_2 from industrial point sources and transporting it to offshore platforms could offer a more feasible route for producing methane and methanol in situ.

4) Among the synthetic fuels studied, ammonia proves to be the most promising. It offers relatively high synthesis efficiency and a small physical footprint, making it more suitable for offshore use. Additionally, ammonia pro- duction can proceed without relying on carbon sources. This paper proposes a novel design that bypasses the need for cryogenic air separation, which further enhances the feasibility of offshore ammonia production.

5) Compressed air storage in the Harald West gas field is constrained to a maximum capacity of 10-20 MW through a single vertical well. This limitation is due to significant pressure drops near the wellbore and restrictions imposed by pipeline infrastructure. More- over, such storage systems require reservoirs with high permeability, such as sandstone or heavily fractured chalk formations, to accommodate large flow rates and mitigate the risk of geomechanically instability.

6) One of the major obstacles to efficient energy recovery in all examined storage methods is the difficulty in retrieving stored fuel at the desired flow rates. This limitation significantly undermines the overall storage efficiency, resulting in extremely low recovery rates (1- 2% in some cases), rendering the process unfeasible for large-scale energy storage.

7) The results suggest that a more controlled and confined storage solution, such as a salt cavern, could be a superior alternative for storing energy in North Sea reservoirs. Salt caverns provide a stable environment for energy storage, reducing the risks of pressure fluctuations and geomechanically instability, and they are better suited for larger-scale operations.

To further enhance the exploration of subsurface energy storage technologies, the simulation tools developed in this study, which integrate Aspen Plus process simulations with subsurface models through a MATLAB script, offer a versatile and automated approach. These tools can be used to

investigate additional energy storage scenarios, refine existing models, and optimize processes for subsurface energy storage, paving the way for more efficient and sustainable energy systems in the future.

REFERENCES

[1] A. Rajkomar, J. Dean, and I. Kohane, "Machine learning in medicine," *New England Journal of Medicine*, vol. 380, no. 14, pp. 1347–1358, 2019.

[2] A. Esteva, B. Kuprel, R. A. Novoa, J. Ko, S. M. Swetter, S. M. Blau, and S. Thrun, "Dermatologist-level classification of skin cancer with deep neural networks," *Nature*, vol. 542, no. 7639, pp. 115–118, 2017.

[3] S. Bauer *et al.*, "Subsurface energy storage: A critical assessment," *Journal of Renewable and Sustainable Energy Reviews*, vol. 28, pp. 137–150, 2013.

[4] A. Bejan, G. Tsatsaronis, and M. Moran, *Thermal Design and Opti- mization*. Wiley-Interscience, 1996.

[5] O. Ellabban, H. Abu-Rub, and F. Blaabjerg, "Renewable energy re- sources: Current status, future prospects, and their enabling technology," *Renewable and Sustainable Energy Reviews*, vol. 39, pp. 748–764, 2014.

[6] IPCC, *Climate Change 2021: The Physical Science Basis, Contribution of Working Group I to the Sixth Assessment Report*. Cambridge University Press, 2021.

[7] O. R. E. Catapult, "North sea wind power hub programme," 2023.

[8] C. McGlade and P. Ekins, "The geographical distribution of fossil fuels unused when limiting global warming to 2°c," *Nature*, vol. 517, no. 7533, pp. 187–190, 2015.

[9] Z. Abdin and A. Zafaranloo, "Overview of power-to-x technology for hydrogen and synthetic fuels," *Renewable Energy and Storage Review*, vol. 34, pp. 423–437, 2020.

[10] N. Heinemann *et al.*, "Enabling large-scale hydrogen storage in porous media," *Nature Communications*, vol. 12, no. 1, pp. 1–13, 2021.

[11] C. Smith, A. K. Hill, and L. Torrente-Murciano, "Current and future role of haber-bosch ammonia in a carbon-free energy landscape," *Energy and Environmental Science*, vol. 13, pp. 331–344, 2020.

[12] A. Keshav and R. Verma, "Ammonia as an energy carrier: A compre- hensive review on storage, transportation, and utilization," *Renewable and Sustainable Energy Reviews*, vol. 134, p. 110349, 2020.

[13] A. Van Der Meer and S. Van Rees, "Exergy-based analysis of com- pressed air energy storage," *Energy Procedia*, vol. 75, pp. 2517–2522, 2015.